Low Emittance Studies for CesrTA

Daniel Gonnella

Department of Physics, Clarkson University, Potsdam, NY, 13699

(Dated: August 6, 2009)

I have studied the effects of Intra-beam and Touschek scattering on lifetime and emittance in the Cornell Electron Storage Ring (CESR). By studying these effects, I can understand more about the machine and its low emittance properties. Also, I have worked to better understand the energy acceptance of the machine, which greatly influences Touschek effects and the lifetime of the particles. The goal is to achieve ultra-low emittance operation which can help contribute to the research underway as part of the CESR Test-Accelerator project. I modified an existing BMAD routine to make it more accurate and developed a data analysis algorithm to handle the large amount of information that is outputted from the program. I then compared the theoretical data I computed with experimental data to judge my computation's accuracy. I found that the acceptance of particles that have suffered an energy change due to Touschek Scattering has a strong dependence on the local lattice functions.

I. INTRODUCTION

The International Linear Collider (ILC) will be the next high energy particle accelerator that is built. It will be an electron-positron collider that will collide beams with energies between 0.25 and 0.5 TeV [1]. The Cornell Electron Storage Ring (CESR) has recently been reconfigured as a test accelerator (CesrTA) for the ILC. CESR is designed in such a way that it is very similar to the ILC's damping rings. These similarities allow research to be done at CESR in order to answer design questions prior to the building of the ILC.

An important design issue for the CesrTA project is that of ultra-low emittance operation. Emittance can be defined as the phase-space area that the particle beam takes up in the ring. Operating at lower emittances will allow for a higher luminosity (the number of particles per unit area per unit time) which will result in more particle interactions during collisions. Since the collisions are the main focus of the ILC, ultra-low emittance operation is essential.

Two effects that I studied that can result in emittance growth are Intra-Beam Scattering (IBS) and the Touschek Effect. IBS results from particles in the beam colliding with one another and scattering in all three dimensions. The Touschek Effect occurs when two particles collide with one another causing the immediate loss of both particles, one with too much energy and the other with too little [2].

The main focus of the research summarized in this paper has been on the Touschek Effect and the Touschek lifetime of the particles. IBS is taken into account but is not analyzed in depth in the scope of this paper. The main theory for the Touschek Effect comes from a paper published by A. Piwinski in 1998 [3]. I based the BMAD routine for my theoretical computations on the theory that Piwinski developed in [3]. BMAD is a library of subroutines used to run simulations of high energy accelerators and storage rings [4]. The most general case for computing Touschek lifetime that is derived in [3] is shown in equation 1. This

general case was used for my calculations.

$$\frac{1}{T_l} = \langle \frac{r_p^2 c N_p}{8\pi\gamma^2\sigma_s\sqrt{\sigma_x^2\sigma_z^2 - \sigma_p^4 D_x^2 D_z^2 \tau_m}} F(\tau_m, B_1, B_2) \rangle \tag{1}$$

where the average is taken over the whole ring. The function, F is defined in equation 2.

$$F(\tau_m, B_1, B_2) = 2\sqrt{\pi(B_1^2 - B_2^2)}\tau_m \int_{\kappa_m}^{\frac{\pi}{2}} ((2\tau + 1)^2(\frac{\frac{\tau}{\tau_m}}{1 + \tau} - 1)/\tau$$

$$+\tau - \sqrt{\tau\tau_m(1 + \tau)} - (2 + \frac{1}{2\tau})\ln\frac{\frac{\tau}{\tau_m}}{1 + \tau})e^{-B_1\tau}I_0(B_2\tau)\sqrt{1 + \tau}\,d\kappa \tag{2}$$

T_l is the Touschek lifetime and the other variables are defined in [3].

By understanding the effects of Touschek Scattering and IBS, we can have a better understanding of what it takes to achieve low-emittance operation and how we can implement it for both the CesrTA project and the ILC. We compare the current dependence of the lifetime and emittance with the theory as developed with these calculations.

II. TOUSCHEK MEASUREMENTS

The Touschek lifetime of a particle is related to the bunch current. The BMAD routine that I worked with originally outputted a file with current and lifetime data. This data is given at different starting points, where the starting point is the zero-current vertical emittance. The routine was modified throughout the research project in order to make it more accurate and to learn more about how the Touschek Effect and Intra-Beam Scattering affects various parameters. First the Touschek lifetime was calculated assuming that IBS does not occur; then, I refined the technique to include these effects. Finally, I modified the routine so that it calculated the following quantities versus the bunch current: horizontal emittance, vertical emittance, energy spread, and bunch length. I tested out the routine using a 2.085 GeV lattice file. The lattice file defines the elements in the machine along with their specific layout and magnetic and electric field properties. After the routine was thoroughly tested, I analyzed data from different lattice files ranging in energy from 1.800 GeV up to 5.000 GeV.

A. No Intra-Beam Scattering

The BMAD routine that is used to calculate the Touschek lifetime of particles is derived from [3]. We know that the lifetime (τ) is related to the current by equation 3:

$$\frac{1}{\tau} = \frac{1}{I}\frac{dI}{dt} \tag{3}$$

Where I is the current and t is the time. Figure 1 shows a plot of data that has been computed using my BMAD routine. It shows the relationship of bunch current to inverse-lifetime, without the effects of IBS. We can see that this relationship is linear.

Since the relationship is linear, we can define the "Touschek parameter" as shown in equation 4.

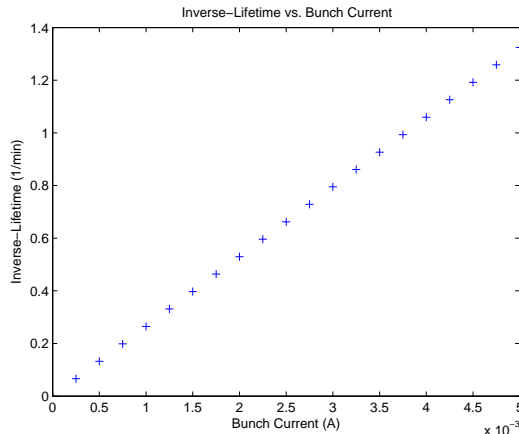$$\frac{1}{\tau} = \frac{1}{b_{touschek}}I + R \tag{4}$$

FIG. 1: Inverse-Lifetime vs. Bunch Current: Effects of IBS are ignored.

Where R is the zero-current inverse-lifetime. To obtain the data shown in figure 1 and other similar data sets, the routine takes a value for the energy acceptance as input. Energy acceptance will be specifically defined in Section III. This inputted value is referred to as the "dynamic" energy acceptance. Measurements done on CESR have suggested that our fractional energy acceptance is somewhere around 0.8%. If the energy acceptance that is given to the routine is less than a computed value, the routine will use the inputted value. Otherwise, it uses a computed value which is shown in equation 5 and comes from Matthew Sands' work in preparing a report on Electron Storage Rings for the U.S. Atomic Energy Commision [5]. This calculation assumes that the acceptance is limited by the depth of the RF bucket and the overvoltage. That is, if a particle falls out of the RF bucket it is lost.

$$(\frac{\epsilon_{max}}{E_0})^2 = \frac{U_0}{\pi \alpha k E_0} F(q) \tag{5}$$

And F is defined as such:

$$F(q) = 2(\sqrt{q^2 - 1} - \arccos \frac{1}{q}) \tag{6}$$

Where ϵ_{max} is the maximum energy aperture, E_0 is the total energy of the particles, U_0 is the energy loss per turn, q is the ratio of peak rf voltage to the minimum voltage required to store an electron, and α is the momentum compaction [5]. The value that our input energy acceptance is compared to is $\frac{\epsilon_{max}}{E_0}$.

The BMAD routine allows for the adjustment of the tune so that different accelerating voltages can be simulated. By looking at different accelerating voltages and energy acceptances, a plot can be generated of the Touschek parameter vs. the accelerating voltage. Figure 2 shows this plot at input acceptances of 0.7, 0.8, 0.9, and 1.0% at approximately 12 and 25 pm zero-current vertical emittances. Without IBS, the vertical emittance will stay constant at the zero-current emittance.

The energy acceptance that is inputted to the routine, however is not accurate enough; it assumes that the acceptance is independent of the location around the ring where the energy change occurs. Section IV will discuss this more in depth but for now, the assumptions about energy acceptance that we have made are reasonable.
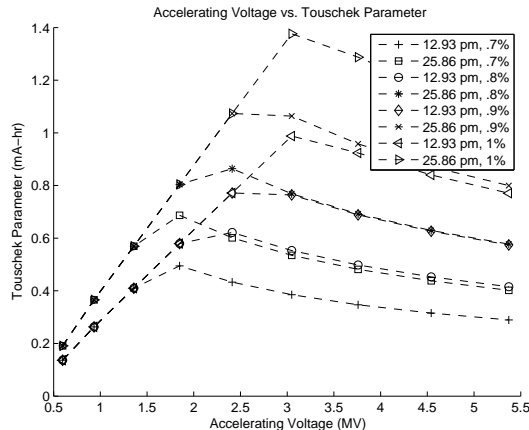
FIG. 2: A plot of the touschek parameter vs. the accelerating voltage for different values of energy acceptance and zero-current vertical emittances.

B.   With Intra-Beam Scattering

A simple modification to the BMAD routine allowed for the effects of IBS to be taken into account. The routine was also modified to output the horizontal emittance, the vertical emittance, the energy spread, and the bunch length. The large amount of data that was outputted by the routine was analyzed using various c++ programs and MATLAB scripts. This allowed for a general algorithm to be developed to analyze data. This technique would be useful when the transition was made from a 2.085 GeV lattice file to others of different energies.

When accounting for IBS, the routine takes a ratio as input. This ratio represents how much of the vertical emittance comes from coupling versus dispersion. A low ratio means that the vertical emittance is dominated by dispersion and a high ratio means it is dominated by coupling. We operate under the assumption that we can accurately compensate for coupling so we use a low ratio. Figure 3 shows a plot of the Touschek parameter with IBS taken into account for a ratio of 0.002. Also, data showing the experimentally obtained Touschek parameter is plotted versus the theoretical plots.

The appendix shows plots of horizontal emittance, vertical emittance, bunch length, and energy spread versus the bunch current. I found that at 2.085 GeV, the horizontal emittance more than doubled as the current was increased from 0 mA to 5 mA. The vertical emittance also increased but not by as large of a factor (Both when using a ratio of 0.2).

Figure 8 in the appendix also shows a plot of the inverse-lifetime versus current while including the IBS effects. It is very similar to figure 1 except that the relation is not as linear. Because of this problem, another, higher order term was added to our approximation. Equation 7 shows this new relationship. Plots of this "c" parameter can be seen in the appendix.

$$\frac{1}{\tau} = \frac{1}{c}I^2 + \frac{1}{b}I + R \tag{7}$$

This paper mainly focuses on the Touschek parameter and the first order approximation. Therefore the computation of the "c" parameter is done for completeness.

As figure 3 shows, the experimental data taken on January 12 and 13, 2009 is close to the theoretical plot of a 0.7% energy acceptance and a zero-current vertical emittance of
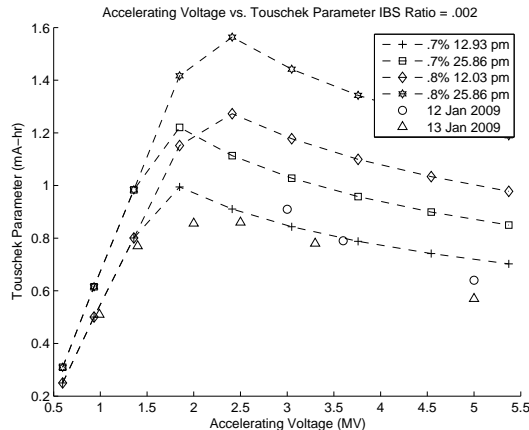
FIG. 3: A plot of the touschek parameter vs. the accelerating voltage with IBS taken into acount for a ratio of 0.002.

12.93 pm. We would like to be even more accurate however, so we move on to discuss the energy acceptance in greater detail.

Other relevent plots and data for other lattice files can be found in [6].

III. DYNAMIC APERTURE ANALYSIS

The energy acceptance needs to be better understood so that we can achieve our goal of ultra-low emittance. By tracking particles in a BMAD simulator, I was able to determine the energy acceptance along the ring. We call this energy acceptance the 0σ energy acceptance; we also will touch on the 4σ energy acceptance. First we discuss the 0σ acceptance.

A. 0σ Energy Acceptance

The 0σ energy acceptance of the machine is the maximum energy change that a particle can receive during Touschek Scattering and not be lost. Using a BMAD routine, I tracked particles around the ring after giving them various initial conditions. They were given an initial horizontal offset and the number of turns to track through. Also, an energy offset was given along with a lattice file to define the machine's properties (including an energy of 2.085 GeV).

Originally the routine was set up so that the tracking would begin at the first element in the ring and then stop. I modified it so that it could track from any starting element. After implementing and testing this loop, I developed the code further to increase the energy offset until the particle was lost. The offset that was given at the point where the particle was lost is the 0σ energy acceptance.

I found that the 0σ acceptance was dependent not only on the size of the energy change but also on the location in the ring that the scatter and resulting energy change occurs. Figure 4 shows this relationship.

This result shows that the energy acceptance is not just dependent on the whole ring as was assumed in the Touschek calculations but is dependent also on the local focusing functions (beta, dispersion, etc.) where the particle loss occurs. We can determine the
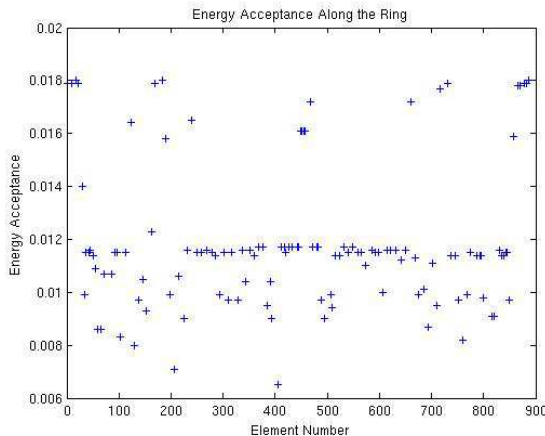
FIG. 4: The 0σ energy acceptance vs. element number

relationship between the acceptance and the local functions by analyzing a particle's motion. As a particle travels along the ring on its stable orbit, it loses energy. This loss causes the particle to have a new stable orbit which it begins to oscillate around. The dispersion and beta functions will also affect this oscillatory motion. The particle's horizontal motion can be described by equation 8.

$$x(s) = \frac{\eta_0 \delta}{\sqrt{\beta_0}} \sqrt{\beta(s)} \cos{(\phi(s) - \phi_0)} + \eta(s)\delta \tag{8}$$

Where δ is the 0σ energy acceptance, $\beta(s)$ is the horizontal beta function at the position s along the ideal orbit, $\eta(s)$ is the dispersion at s, and β_0 and η_0 are the beta function and dispersion where the scatter occurs, respectively. We can then define the energy acceptance to be proportional to a function of beta and dispersion as shown in equation 9. This derivation is shown more in-depth in Section IV.

$$\delta \sim \frac{1}{\eta_0 \sqrt{\frac{\beta_{max}}{\beta_0}} + \eta_{max}} \tag{9}$$

Figure 5 shows this relationship. It can be seen that there is a direct relationship but it is very noisy which suggests that we are missing some other dependence. It should be however, more accurate than our previous model, since it does not assume that the acceptance is the same everywhere along the ring.

B. 4σ Energy Acceptance

The 4σ energy acceptance can be defined as the lowest energy offset a particle can have without having its horizontal position larger than 4σ, in which case it would be lost. The process for determining the 4σ acceptance was similar to finding the 0σ acceptance except that the energy offset is decreased as opposed to increased. I found that, like the 0σ acceptance, the 4σ acceptance was dependent on the local focusing functions as well as the whole ring.
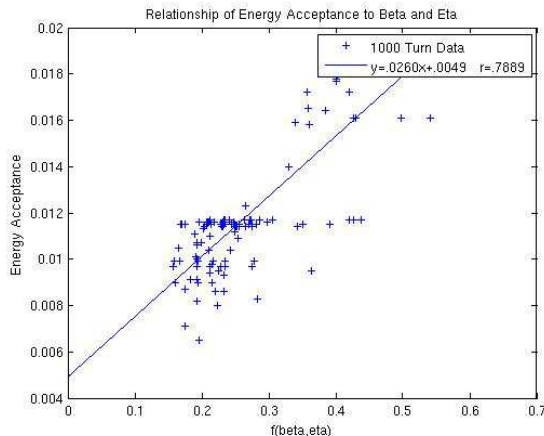
FIG. 5: Relationship of energy acceptance to local focusing functions as defined in equation 9.

Since the Touschek calculation does not emphasize the 4σ energy acceptance, it is only necessary to understand that this acceptance is dependent on the individual elements, similar to the 0σ acceptance.

IV. COMBINING DYNAMIC APERTURE AND TOUSCHEK CALCULATIONS

With a better understanding of the energy acceptance and its dependence on the local focusing functions, we can implement a more accurate BMAD routine for calculating the Touschek lifetime of particles. While the experimentally obtained Touschek parameters suggest an effective value for the energy acceptance of 0.7%, calculation of energy acceptance by tracking from only a zero-dispersion point in the lattice suggests an energy acceptance of approximately 1.80%.

By ignoring the cosine term from equation 8, we can simplify and derive an expression for $x(s)$ and its relationship to the machine's aperture. This is shown in equation 10.

$$x(s) = \delta(\eta_0\sqrt{\frac{\beta_{max}}{\beta_0}} + \eta_{max}) < x_{ap} \tag{10}$$

By solving for δ, we can see the relationship from 9 as an equality.

$$\delta = \frac{x_{ap}}{\eta_0\sqrt{\frac{\beta_{max}}{\beta_0}} + \eta_{max}} \tag{11}$$

Where x_{ap} represents the physical aperture of the machine. Note that this physical aperture is not known, it was calculated by plotting data from 9 and fitting to a linear curve. After implementing this new energy acceptance into the Touschek routine, we compared its output with output from the old routine (which used an energy acceptance of 0.8% throughout the entire ring). Figure 6 shows this comparison.

There is a significant difference between the data using 0.8% and the data that uses the more advanced method for calculating energy acceptance. By comparing plots of constant energy acceptances to the new computed data, we can determine a more accurate value for our "effective" energy acceptance. Figure 7 shows this comparison. The new method's
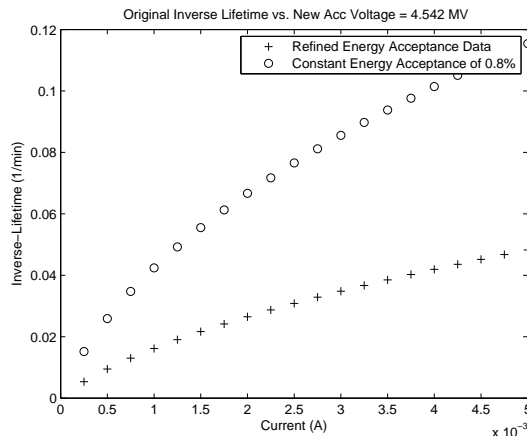
FIG. 6: A comparison of the data outputted using the refined energy acceptance and data using a constant 0.8 energy acceptance.

output closely follows the data for a 1.15% constant energy acceptance which shows that the "effective" energy acceptance is approximately 1.15%. This effective aperture of 1.15% is almost certainly an overestimate since it is consistent with measurements only if we assume a very small zero-current vertical emittance. Although this still differs from the experimental data's suggestion of 0.7%, it is much more likely than our single-point estimate of 1.80%.
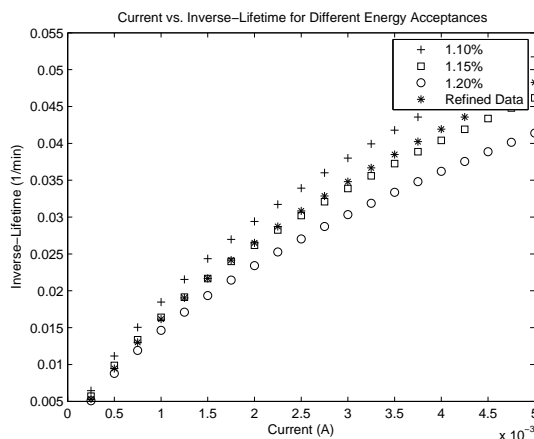
FIG. 7: A comparison of various constant energy acceptances to the more accurate model.

V. CONCLUSIONS

The Touschek lifetime of particles is greatly dependent on the accelerating voltage and beam energy. It also depends on the energy acceptance of the machine, which is not just a property of the size of the energy change during the collision but also on where the scatter occurs. The "energy acceptance" (size of the energy change) can be defined as a function of the local focusing functions (beta, dispersion, etc.), as opposed to being a constant for the whole machine as was previously assumed.

By implementing this new method for computing Touschek lifetime, we have found that the "effective" energy acceptance is approximately 1.15%. This still disagrees with our experimentally obtained Touschek parameters which suggest an energy acceptance of approximately 0.7%, however this difference could be a result of non-linearities that were not taken into account in the calculation. Focusing magnets and other elements have certain non-linearites that were ignored for simplicity. Future research may be devoted to refining this technique further and accounting for the non-linearities. Most importantly, these results can help us to understand the properties of CESR so that we are better able to achieve ultra-low emittance.

Acknowledgements

[1] M. Ehrlichman "Design Studies for the Proposed CESR Accelerator Test Facility"

[2] Chao, A. and Tigner, M. *Handbook of Accelerator Physics and Engineering*, 1999

[3] A. Piwinski "The Touschek Effect in Strong Focusing Storage Rings" DESY 98-179, 1998

[4] *BMAD Subroutine Library for Relativistic Charged-Particle Simulations*, This source can be found at http://www.lns.cornell.edu/~dcs/bmad/

[5] Sands, M. *The Physics of Electron Storage Rings: An Introduction*, SLAC-121, 1970

[6] Gonnella, D. *Dan Gonnella's REU Page* Found at http://www.lepp.cornell.edu/~gonnelda/

Appendix

More plots can be found at [6]. The following plots were made using a ratio of 0.2, implying that more of the vertical emittance comes from dispersion than from coupling.
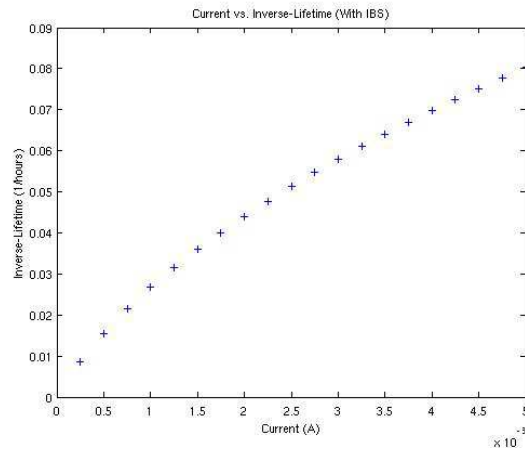

FIG. 8: A plot of the inverse-lifetime vs. the bunch current with IBS effects included.
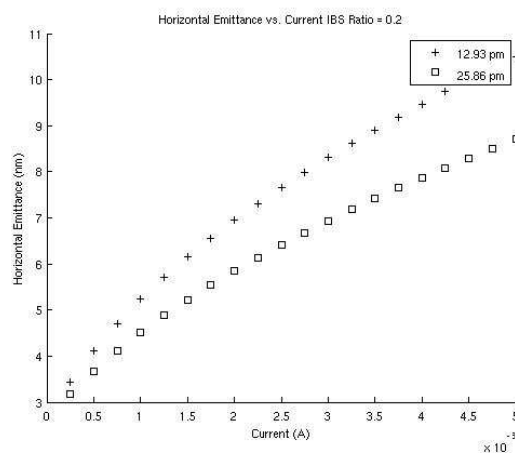

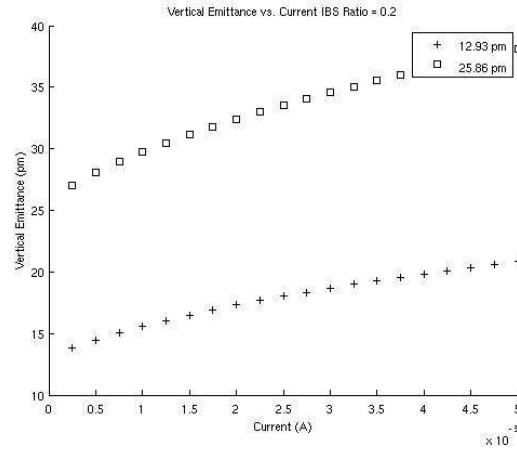FIG. 9: A plot of horizontal emittance vs. bunch current
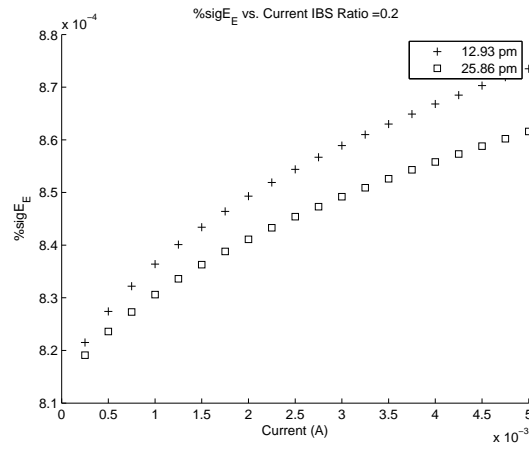
FIG. 10: A plot of vertical emittance vs. bunch current

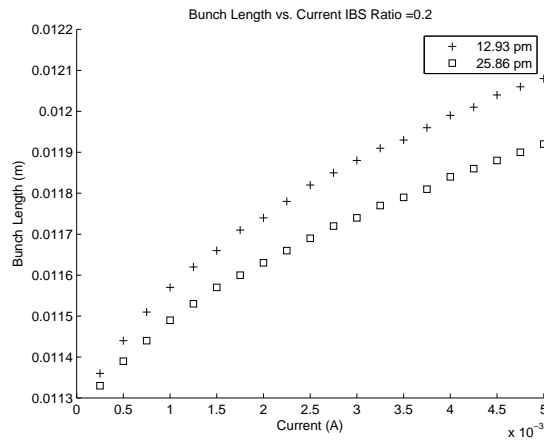FIG. 11: A plot of energy spread vs. bunch current

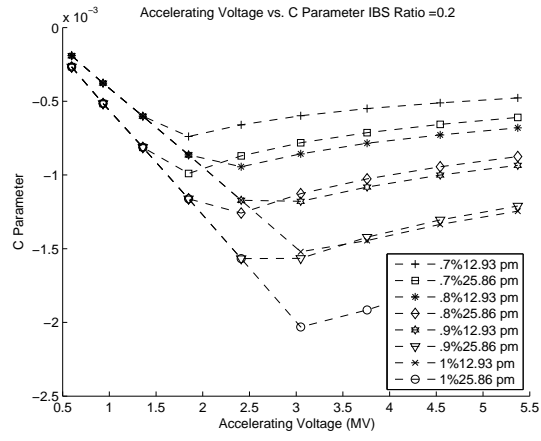

FIG. 12: A plot of bunch length vs. bunch current

FIG. 13: A plot of the c parameter vs. accelerating voltage